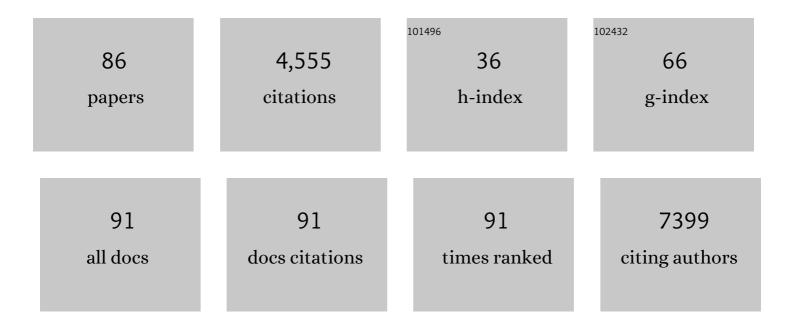
List of Publications by Year in descending order

Source: https://exaly.com/author-pdf/9207452/publications.pdf Version: 2024-02-01



#	Article	IF	CITATIONS
1	Gold Nanorodâ^'Photosensitizer Complex for Near-Infrared Fluorescence Imaging and Photodynamic/Photothermal Therapy <i>In Vivo</i> . ACS Nano, 2011, 5, 1086-1094.	7.3	710
2	Sensing Phosphatase Activity by Using Gold Nanoparticles. Angewandte Chemie - International Edition, 2007, 46, 707-709.	7.2	241
3	Gold and Hairpin DNA Functionalization of Upconversion Nanocrystals for Imaging and In Vivo Drug Delivery. Advanced Materials, 2017, 29, 1700244.	11.1	186
4	Selective Antitumor Effect of Novel Protease-Mediated Photodynamic Agent. Cancer Research, 2006, 66, 7225-7229.	0.4	161
5	Porous platinum nanoparticles as a high-Z and oxygen generating nanozyme for enhanced radiotherapy in vivo. Biomaterials, 2019, 197, 12-19.	5.7	152
6	A fluorescent turn-on probe for the detection of alkaline phosphatase activity in living cells. Chemical Communications, 2011, 47, 9825.	2.2	146
7	Developing a Peptide-Based Near-Infrared Molecular Probe for Protease Sensing. Bioconjugate Chemistry, 2004, 15, 1403-1407.	1.8	145
8	A boronate-based fluorescent probe for the selective detection of cellular peroxynitrite. Chemical Communications, 2014, 50, 9353-9356.	2.2	113
9	ROS-Responsive Activatable Photosensitizing Agent for Imaging and Photodynamic Therapy of Activated Macrophages. Theranostics, 2014, 4, 1-11.	4.6	112
10	A mitochondrial targeted fusion peptide exhibits remarkable cytotoxicity. Molecular Cancer Therapeutics, 2006, 5, 1944-1949.	1.9	108
11	A BODIPYâ€Based Probe for the Selective Detection of Hypochlorous Acid in Living Cells. Chemistry - an Asian Journal, 2011, 6, 1358-1361.	1.7	107
12	A ratiometric fluorescent probe based on a BODIPY–DCDHF conjugate for the detection of hypochlorous acid in living cells. Analyst, The, 2013, 138, 3368.	1.7	103
13	Visualization of tyrosinase activity in melanoma cells by a BODIPY-based fluorescent probe. Chemical Communications, 2011, 47, 12640.	2.2	90
14	Photosensitizer-Conjugated Gold Nanorods for Enzyme-Activatable Fluorescence Imaging and Photodynamic Therapy. Theranostics, 2012, 2, 190-197.	4.6	90
15	Graphene oxide–photosensitizer conjugate as a redox-responsive theranostic agent. Chemical Communications, 2012, 48, 9912.	2.2	88
16	Theranostic nanosystems for targeted cancer therapy. Nano Today, 2018, 23, 59-72.	6.2	86
17	Recent advances in nanoparticle carriers for photodynamic therapy. Quantitative Imaging in Medicine and Surgery, 2018, 8, 433-443.	1.1	85
18	A graphene oxide–photosensitizer complex as an enzyme-activatable theranostic agent. Chemical Communications. 2013. 49. 1202.	2.2	72

#	Article	IF	CITATIONS
19	Conjugation of a Photosensitizer to an Oligoarginine-Based Cell-Penetrating Peptide Increases the Efficacy of Photodynamic Therapy. ChemMedChem, 2006, 1, 458-463.	1.6	65
20	Gold nanorods for target selective SPECT/CT imaging and photothermal therapy in vivo. Quantitative Imaging in Medicine and Surgery, 2012, 2, 1-11.	1.1	65
21	Hyaluronic acid–polypyrrole nanoparticles as pH-responsive theranostics. Chemical Communications, 2014, 50, 15014-15017.	2.2	63
22	Effects of Gold Nanorod Concentration on the Depthâ€Related Temperature Increase During Hyperthermic Ablation. Small, 2011, 7, 265-270.	5.2	56
23	Preparation and Characterization of Water/Oil/Water Emulsions Stabilized by Polyglycerol Polyricinoleate and Whey Protein Isolate. Journal of Food Science, 2010, 75, E116-25.	1.5	54
24	Photosensitizer-conjugated polymeric nanoparticles for redox-responsive fluorescence imaging and photodynamic therapy. Journal of Materials Chemistry B, 2013, 1, 429-431.	2.9	54
25	Mesoporous silica-based nanoplatforms for the delivery of photodynamic therapy agents. Journal of Pharmaceutical Investigation, 2018, 48, 3-17.	2.7	54
26	Redox-Responsive Manganese Dioxide Nanoparticles for Enhanced MR Imaging and Radiotherapy of Lung Cancer. Frontiers in Chemistry, 2017, 5, 109.	1.8	53
27	Fucoidan-Based Theranostic Nanogel for Enhancing Imaging and Photodynamic Therapy of Cancer. Nano-Micro Letters, 2020, 12, 47.	14.4	53
28	Long-term delivery of all-trans-retinoic acid using biodegradable PLLA/PEG-PLLA blended microspheres. International Journal of Pharmaceutics, 2001, 215, 67-81.	2.6	52
29	A New Strategy for Fluorogenic Esterase Probes Displaying Low Levels of Nonâ€specific Hydrolysis. Chemistry - A European Journal, 2015, 21, 9645-9649.	1.7	52
30	Polyethylene Glycol (PEG) Modified 99mTc-HMPAOLiposome for Improving Blood Circulation and Biodistribution: The Effect of the Extent of PEGylation. Cancer Biotherapy and Radiopharmaceuticals, 2005, 20, 620-628.	0.7	49
31	Photodynamic Therapy Using a Protease-Mediated Theranostic Agent Reduces Cathepsin-B Activity in Mouse Atheromata In Vivo. Arteriosclerosis, Thrombosis, and Vascular Biology, 2013, 33, 1360-1365.	1.1	48
32	Targeted, Stimuli-Responsive, and Theranostic ¹⁹ F Magnetic Resonance Imaging Probes. Bioconjugate Chemistry, 2019, 30, 2502-2518.	1.8	46
33	A folate receptor-specific activatable probe for near-infrared fluorescence imaging of ovarian cancer. Chemical Communications, 2014, 50, 7507-7510.	2.2	45
34	Hydroxychloroquine-loaded hollow mesoporous silica nanoparticles for enhanced autophagy inhibition and radiation therapy. Journal of Controlled Release, 2020, 325, 100-110.	4.8	43
35	Smart dual-functional warhead for folate receptor-specific activatable imaging and photodynamic therapy. Chemical Communications, 2014, 50, 10600-10603.	2.2	41
36	Electroactive Polypyrrole Nanowire Arrays: Synergistic Effect of Cancer Treatment by On-Demand Drug Release and Photothermal Therapy. Langmuir, 2015, 31, 4264-4269.	1.6	41

#	Article	IF	CITATIONS
37	Indocyanine green-loaded hollow mesoporous silica nanoparticles as an activatable theranostic agent. Nanotechnology, 2017, 28, 185102.	1.3	38
38	Indocyanine green-loaded perfluorocarbon nanoemulsions for bimodal (19)F-magnetic resonance/nearinfrared fluorescence imaging and subsequent phototherapy. Quantitative Imaging in Medicine and Surgery, 2013, 3, 132-40.	1.1	35
39	Protease-Mediated Phototoxicity of a Polylysine–Chlorine6 Conjugate. ChemMedChem, 2006, 1, 698-701.	1.6	32
40	Inhibition of tumor growth by biodegradable microspheres containing all-trans-retinoic acid in a human head-and-neck cancer xenograft. International Journal of Cancer, 2003, 107, 145-148.	2.3	31
41	Theranostic nanoparticles for enzyme-activatable fluorescence imaging and photodynamic/chemo dual therapy of triple-negative breast cancer. Quantitative Imaging in Medicine and Surgery, 2015, 5, 656-64.	1.1	31
42	Membrane permeable esterase-activated fluorescent imaging probe. Bioorganic and Medicinal Chemistry Letters, 2007, 17, 5054-5057.	1.0	30
43	Effects of enzymatically modified starch on the encapsulation efficiency and stability of water-in-oil-in-water emulsions. Food Chemistry, 2011, 128, 266-275.	4.2	28
44	A novel endoscopic fluorescent clip for the localization of gastrointestinal tumors. Surgical Endoscopy and Other Interventional Techniques, 2011, 25, 2372-2377.	1.3	25
45	Heparin-based self-assembled nanoparticles for photodynamic therapy. Macromolecular Research, 2011, 19, 487-494.	1.0	25
46	Poly(ethylene glycol)–poly(l-lactide) diblock copolymer prevents aggregation of poly(l-lactide) microspheres during ethylene oxide gas sterilization. Biomaterials, 2001, 22, 995-1004.	5.7	23
47	Polypyrrole-based nanotheranostics for activatable fluorescence imaging and chemo/photothermal dual therapy of triple-negative breast cancer. Nanotechnology, 2016, 27, 185102.	1.3	23
48	Fluorescence imaging of spatial location of lipids and proteins during digestion of protein-stabilized oil-in-water emulsions: A simulated gastrointestinal tract study. Food Chemistry, 2017, 219, 297-303.	4.2	23
49	Responsive alginate-cisplatin nanogels for selective imaging and combined chemo/radio therapy of proliferating macrophages. Quantitative Imaging in Medicine and Surgery, 2018, 8, 733-742.	1.1	23
50	Implications of Web of Science journal impact factor for scientific output evaluation in 16 institutions and investigators' opinion. Quantitative Imaging in Medicine and Surgery, 2014, 4, 453-61.	1.1	23
51	Multivalent mannose-decorated NIR nanoprobes for targeting pan lymph nodes. Chemical Engineering Journal, 2018, 340, 51-57.	6.6	22
52	meso-ester BODIPYs for the imaging of hypoxia in tumor cells. Sensors and Actuators B: Chemical, 2017, 249, 229-234.	4.0	20
53	A highly sensitive magnetite nanoparticle as a simple and rapid stem cell labelling agent for MRI tracking. Journal of Materials Chemistry, 2011, 21, 7742.	6.7	19
54	Photoactivatable BODIPY Platform: Light-Triggered Anticancer Drug Release and Fluorescence Monitoring. ACS Applied Bio Materials, 2019, 2, 2567-2572.	2.3	19

#	Article	IF	CITATIONS
55	Influence of environmental stresses on the stability of W/O/W emulsions containing enzymatically modified starch. Carbohydrate Polymers, 2013, 92, 1503-1511.	5.1	17
56	Chemoprevention of 4-NQO-induced oral carcinogenesis by co-administration of all-trans retinoic acid loaded microspheres and celecoxib. Journal of Controlled Release, 2005, 104, 167-179.	4.8	16
57	Molecular Imaging: From Bench to Clinic. BioMed Research International, 2014, 2014, 1-3.	0.9	16
58	A redox-responsive theranostic agent for target-specific fluorescence imaging and photodynamic therapy of EGFR-overexpressing triple-negative breast cancers. Journal of Materials Chemistry B, 2016, 4, 6787-6790.	2.9	16
59	CD44v8-10 as a potential theranostic biomarker for targeting disseminated cancer cells in advanced gastric cancer. Scientific Reports, 2017, 7, 4930.	1.6	16
60	Indocyanine green-loaded injectable alginate hydrogel as a marker for precision cancer surgery. Quantitative Imaging in Medicine and Surgery, 2020, 10, 779-788.	1.1	15
61	Release properties of gel-type W/O/W encapsulation system prepared using enzymatically-modified starch. Food Chemistry, 2014, 157, 77-83.	4.2	14
62	Antigen-responsive molecular sensor enables real-time tumor-specific imaging. Theranostics, 2017, 7, 952-961.	4.6	14
63	Rapid tissue histology using multichannel confocal fluorescence microscopy with focus tracking. Quantitative Imaging in Medicine and Surgery, 2018, 8, 884-893.	1.1	14
64	Lipase digestibility of the oil phase in a water-in-oil-in-water emulsion. Food Science and Biotechnology, 2015, 24, 513-520.	1.2	13
65	A Quenched Annexin Vâ€Fluorophore for the Realâ€Time Fluorescence Imaging of Apoptotic Processes In Vitro and In Vivo. Advanced Science, 2020, 7, 2002988.	5.6	13
66	Photosensitizer-complexed polypyrrole nanoparticles for activatable fluorescence imaging and photodynamic therapy. Journal of Materials Chemistry B, 2016, 4, 7545-7548.	2.9	12
67	In vivo biocompatibility studies of poly(D,L-lactide)/poly(ethylene glycol)-poly(L-lactide) microspheres containing all-trans-retinoic acid. Journal of Biomaterials Science, Polymer Edition, 2002, 13, 301-322.	1.9	11
68	Enhanced Fluorescence Imaging and Photodynamic Cancer Therapy Using Hollow Mesoporous Nanocontainers. Chemistry - an Asian Journal, 2017, 12, 1700-1703.	1.7	11
69	A redox-responsive folate–fluorophore conjugate as a new target-cell-specific imaging probe. Journal of Materials Chemistry B, 2018, 6, 2524-2527.	2.9	10
70	Zwitterionic near-infrared fluorophore-conjugated epidermal growth factor for fast, real-time, and target-cell-specific cancer imaging. Theranostics, 2019, 9, 1085-1095.	4.6	10
71	Atorvastatin and clopidogrel interfere with photosensitization in vitro. Photochemical and Photobiological Sciences, 2011, 10, 1587.	1.6	9
72	Fluorometric sensing of intracellular thiols in living cells using a AuNPs/1-PR3+ adsorbate. Sensors and Actuators B: Chemical, 2013, 177, 467-471.	4.0	9

#	Article	IF	CITATIONS
73	A novel endoscopic fluorescent band ligation method for tumor localization. Surgical Endoscopy and Other Interventional Techniques, 2016, 30, 4659-4663.	1.3	9
74	Mini-Platform for Off–On Near-Infrared Fluorescence Imaging Using Peptide-Targeting Ligands. Bioconjugate Chemistry, 2020, 31, 721-728.	1.8	9
75	Ubiquinone-BODIPY nanoparticles for tumor redox-responsive fluorescence imaging and photodynamic activity. Journal of Materials Chemistry B, 2021, 9, 824-831.	2.9	9
76	Photosensitizer-conjugated tryptophan-containing peptide ligands as new dual-targeted theranostics for cancers. International Journal of Pharmaceutics, 2016, 513, 584-590.	2.6	8
77	Subacute toxicity of all-trans-retinoic acid loaded biodegradable microspheres in rats. Drug Development Research, 2003, 59, 326-332.	1.4	5
78	Chemopreventive efficacy of all-trans-retinoic acid in biodegradable microspheres against epithelial cancers: Results in a 4-nitroquinoline 1-oxide-induced oral carcinogenesis model. International Journal of Pharmaceutics, 2006, 320, 45-52.	2.6	5
79	Quenched cetuximab conjugate for fast fluorescence imaging of EGFR-positive lung cancers. Biomaterials Science, 2021, 9, 456-462.	2.6	5
80	Inhibition effect of new farnesol derivatives on all-trans-retinoic acid metabolism. Metabolism: Clinical and Experimental, 2001, 50, 1356-1360.	1.5	4
81	Effects of ethylene oxide gas sterilization on physical properties of poly(L-lactide)–poly(ethylene) Tj ETQq1 1 0. 783-799.	784314 r 1.9	gBT /Overloc 4
82	Methods of Hematoxylin and Erosin Image Information Acquisition and Optimization in Confocal Microscopy. Healthcare Informatics Research, 2016, 22, 238.	1.0	2
83	Rapid histologic diagnosis using quick fluorescence staining and tissue confocal microscopy. Microscopy Research and Technique, 2019, 82, 892-897.	1.2	2
84	Acute toxicity of all-trans-retinoic acid loaded poly(L-lactide)/poly(ethylene glycol)-poly(L-lactide) microspheres in mice. Drug Development Research, 2002, 57, 134-139.	1.4	0
85	Augmentation of all-trans-retinoic acid concentration in plasma by preventing inflammation responses induced by atRA-loaded microspheres with concurrent treatment of dexamethasone. Drug Development Research, 2004, 61, 197-206.	1.4	0
86	Realâ€Time Apoptosis Imaging: A Quenched Annexin Vâ€Fluorophore for the Realâ€Time Fluorescence Imaging of Apoptotic Processes In Vitro and In Vivo (Adv. Sci. 24/2020). Advanced Science, 2020, 7, 2070137.	5.6	0